Third International Conference on Sustainable Construction Materials and Technologies http://www.claisse.info/Proceedings.htm

# Development of Steel Slag Hydrated Matrix with Anti-Washout Performance

Takumi Sawada[1,*], Tetsuya Ogasawara[1], Yoshihiro Takano[2], Hiroki Kanno[3], Yohsuke Yamagoshi[2] and Tadashi Imamura[4]

[1]*Penta-Ocean Construction Institute of Technology, Japan*
[2]*Nippon Steel & Sumitomo Metal Corporation, Plant Engineering and Facility Management Center, Japan*
[3]*Nippon Steel & Sumitomo Metal Corporation, Nagoya Works, Japan*
[4]*Penta-Ocean Construction, Nagoya Branch, Construction Work Office, Japan*
[*]*1534-1, Yonku-cho, Nasushiobara-shi, Tochigi-ken 329-2746, Japan.*
*E-mail: <Takumi.Sawada@mail.penta-ocean.co.jp>, <Tetsuya. Ogasawara@mail.penta-ocean.co.jp>, <takano.e5a.yoshihiro@jp.nssmc.com>, <kanno.7fz.hiroki@jp.nssmc.com>, <yamagoshi.6kg.yohsuke@jp.nssmc.com>, <Tadashi.A.Imamura@mail.penta-ocean.co.jp>.*

## ABSTRACT

This paper reports the development of a steel slag hydrated matrix with anti-washout performance, with the goal of sustainable development of society. For the development of the matrix, both laboratory experiments and trial construction were carried out. Furthermore, the carbon-dioxide emissions originating in the composition material were calculated. It was confirmed that steel slag hydrated matrix with anti-washout performance has sufficient characteristic to use in construction and greatly reduces carbon-dioxide emissions.

**Keywords.** Steel-making Slag, Ground Granulated Blast-Furnace Slag, Hydrated Matrix, Carbon Dioxide, Anti-washout

## INTRODUCTION

In various industries, reduction of the environmental impact is needed to maintain sustainable development. In the construction and manufacturing industries, a new steel slag hydrated matrix material is proposed to contribute to the reduction of the environmental impact of industrial wastes. The steel slag hydrated matrix is manufactured by mixing steel-making slag and ground granulated blast-furnace slag powder, which are by-products of the manufacture of iron; some alkaline activator (ordinary Portland cement or Portland blast-furnace slag cement was used in the present study) is added if needed. This material has a strength equivalent to that of concrete after a hydration reaction.

The purpose of this study is to expand the applicability of the steel slag hydrated matrix. In this study, anti-washout performance under water is realized for the steel slag hydrated matrix by improving the mix proportions and adding an anti-washout admixture. This paper presents the results of a laboratory experiment and trial construction, and an estimate of the carbon-dioxide emissions. The performance of the matrix in fresh conditions, such as the

slump flow and degree of underwater segregation, and the performance in a solidified condition, such as strength and volume changes, were investigated in laboratory experiments. Flatness without vibrating and flow inclination were investigated in the trial construction. From the estimate of carbon-dioxide emissions, those originating in composition material were calculated.

## STEEL-MAKING SLAG

Steel-making slag is an inorganic substance, of which CaO and $SiO_2$ are the main ingredients. It is generated during the steel-making process of refining molten iron, scrap, etc., and has high toughness and processability. Generally, it resembles crushed stone, and is an indispensable ingredient of the steel slag hydrated matrix, in which it used as a material equivalent to fine aggregates or coarse aggregates. Moreover, it works also as alkaline activator that accelerates the hydration reaction of ground granulated blast-furnace slag powder. The slag A ($SG_A$, $SS_A$) or B ($SG_B$, $SS_B$) was used in the present study. An example of the quality test results of each slag and the standard value from an engineering manual of the steel slag hydrated matrix are shown in **Table 1** and **Figure 1**.

**Table 1. Quality of steel-making slag**

| Item | Unit | Standard value | A | | B | |
|---|---|---|---|---|---|---|
| | | | $SG_A$ | $SS_A$ | $SG_B$ | $SS_B$ |
| Maximum size | mm | ≤25 | 25 | 5 | 25 | 5 |
| MgO | % | ≤8.5 | 3.17 | 3.13 | 5.06 | |
| S | % | ≤2.0 | 0.46 | 0.53 | 0.062 | |
| Fe | % | - | - | - | 1.76 | |
| Powdering ratio | % | ≤2.5 | 0.40 | 0.49 | 0.2–0.5 | |
| Saturated and surface-dry particle density | g/cm$^3$ | - | 3.08 | 2.82 | 3.13 | 3.01 |
| Oven-dry particle density | g/cm$^3$ | 2.6≤ | 2.94 | 2.65 | 3.07 | 2.85 |
| Water absorption | % | - | 3.78 | 6.22 | 1.99 | 5.63 |
| Particles passing standard sieve size of 75 μm | % | - | 2.0 | 14.2 | - | 9.8 |
| Fineness modulus | - | - | 6.40 | 3.04 | 6.71 | 3.04 |

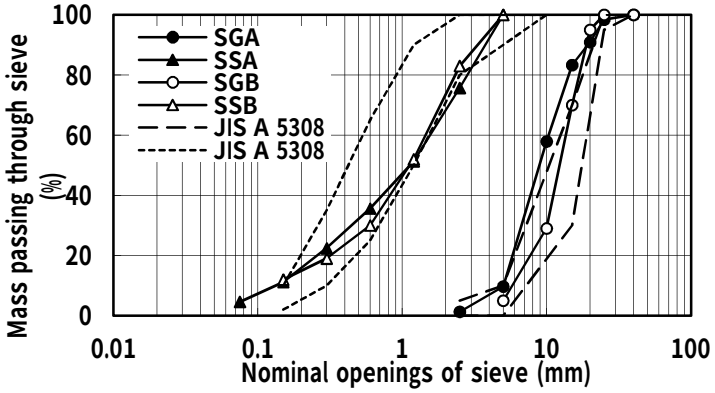


**Figure 1. Particle-size accumulation curve of steel-making slag**

## MATERIALS

The properties of the materials used in this study are listed in **Table 2**.

**Table 2. Properties of materials**

| Sign | Properties |
|---|---|
| W | Service water |
| OPC | Ordinary Portland cement (density: 3.16 g/cm$^3$, specific surface area: 3340 cm$^2$/g) |
| BB | Portland blast-furnace slag cement B (density: 3.04 g/cm$^3$, specific surface area: 3820 cm$^2$/g, replacement by BP ratio: 47%) |
| $BP_A$ | Ground granulated blast-furnace slag powder (density: 2.91 g/cm$^3$, specific surface area: 4120 cm$^2$/g) |
| $BP_B$ | Ground granulated blast-furnace slag powder (density: 2.89 g/cm$^3$, specific surface area: 4200 cm$^2$/g) |
| $SG_x$ | Steel-making slag coarse aggregate (cf. Table 1, Fig. 1) |
| $SS_x$ | Steel-making slag fine aggregate (cf. Table 1, Fig. 1) |
| SP | Air-entraining and high-range water-reducing admixture |
| Vi | Anti-washout admixture |

## MIX PROPORTIONS

Eleven mix proportions were set up by trial mixes in the present study. The cases whose names begin with the letter "A" have a nominal strength of 18–30 N/mm$^2$ and a slump flow of approximately 50 cm. The cases whose names begin with the letter "B" have a nominal strength of 18 N/mm$^2$ and a slump flow of approximately 55 cm. The list of mix proportions is given in **Table 3**. In addition, SS and pH, which indicate the degree of underwater segregation in the method given in JSCE-D104, are within the limits of 50 mg/L or less and 12.0 or less. Moreover, the strength index and alkaline activator ratio are defined as in formulas (1)–(3).

**Table 3. Mix proportions**

| Case | Strength index | Alkaline activator ratio (%) | Unit weight (kg/m$^3$) | | | | | | Admixture | | Test result | |
|---|---|---|---|---|---|---|---|---|---|---|---|---|
| | | | W | BP | OPC | BB | SS | SG | SP (C×%) | Vi (W×%) | SF (mm) | Air (%) |
| A2.1-15 | 2.1 | 15 | 250 | 388 | 69 | - | 809 | 886 | 2.00 | 1.10 | 525 | 1.9 |
| A2.6-10 | 2.6 | 10 | 255 | 543 | 60 | - | 733 | 800 | 2.00 | 1.10 | 520 | 2.0 |
| A2.6-15 | 2.6 | 15 | 255 | 490 | 87 | - | 747 | 815 | 2.00 | 1.10 | 515 | 1.9 |
| A2.6-25 | 2.6 | 25 | 255 | 398 | 133 | - | 770 | 842 | 2.00 | 1.10 | 505 | 2.0 |
| A3.1-15 | 3.1 | 15 | 260 | 596 | 105 | - | 680 | 743 | 2.00 | 1.10 | 500 | 2.2 |
| B1.3-15 | 1.3 | 15 | 250 | 203 | - | 80 | 851 | 1082 | 2.00 | 1.10 | 545 | 2.2 |
| B1.8-0 | 1.8 | 0 | 250 | 450 | - | - | 771 | 980 | 2.00 | 1.10 | 580 | 2.6 |
| B1.8-5 | 1.8 | 5 | 250 | 388 | - | 40 | 782 | 994 | 2.00 | 1.10 | 570 | 2.4 |
| B1.8-15 | 1.8 | 15 | 250 | 281 | - | 111 | 801 | 1018 | 2.00 | 1.10 | 540 | 2.0 |
| B1.8-25 | 1.8 | 25 | 250 | 190 | - | 170 | 817 | 1039 | 2.00 | 1.10 | 520 | 2.3 |
| B2.3-15 | 2.3 | 15 | 250 | 358 | - | 142 | 751 | 954 | 2.00 | 1.10 | 530 | 2.1 |

Strength index = BP + 2NP (1)

Alkaline activator ratio = NP/(OPC + BB + BP) (2)

NP = OPC = 0.53BB (3)

## TEST RESULTS

**Mechanical properties**. **Figure 2** shows the compressive strength of the specimen made in air and the development of the compressive strength in the case that uses blast-furnace slag cement B indicated by standard specifications for the "design" of concrete structures by JSCE. The ratios of the strengths in water to those in air at 28 days are shown in **Figure 3**. The relationships of the compressive strength and the Young's modulus of the "A" specimen with the calculated values are shown in **Figure 4**. The values are calculated by standard specifications for the "design" of concrete structures by JSCE and compensated in this study.

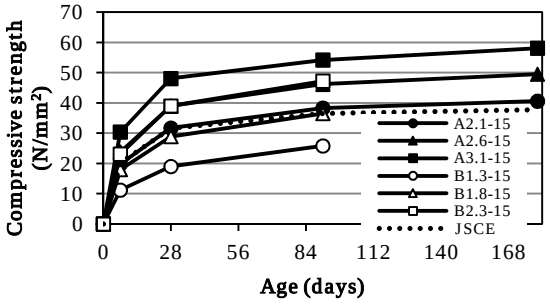


**Figure 2. Compressive strength**

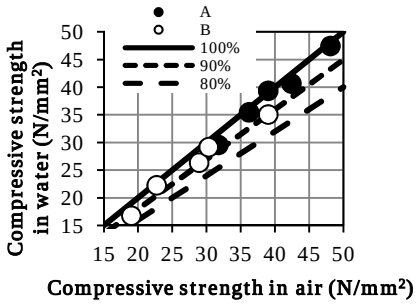


**Figure 3. Ratio of strengths in water and air**

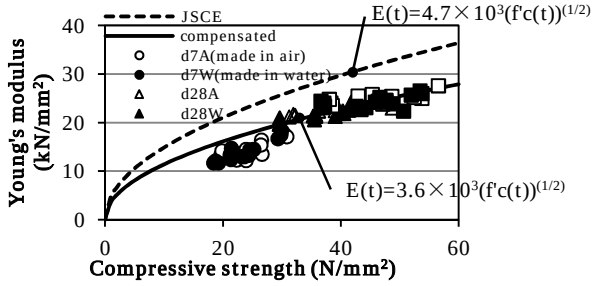


**Figure 4. Young's modulus**

The compressive strength increases until six months. The results shown in **Figures 2** and **3** are the means of three specimens. The difference for every test specimen was ±5% at the maximum. From the observation of **Figure2**, it is expected that the development of the compressive strength will be almost the same as that of concrete that uses blast-furnace slag cement B. The ratio of strengths in water and air was approximately 90 to 100%. Although this ratio exceeded 100% for some of the cases, the cause for this is unknown at present. Regarding the Young's modulus, there was no difference between the specimens made in water and air. Generally, the Young's modulus was less than the calculated value according to the expression of relations of compressive strength and Young's modulus shown in standard specifications for concrete structures. The test values were approximately 75% of the calculated values. Moreover, at 7 days, test values were still lower.

**Alkaline activator ratio**. For the cases where the strength indexes are 2.6 and 1.8, the relationship between the compressive strength of the specimens made in air at 28 days and the alkaline activator ratio is shown in **Figure 5**.

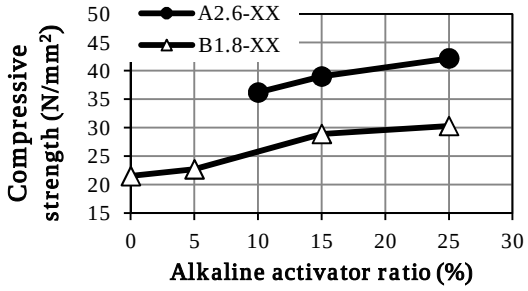


**Figure 5. Relationship between compressive strength and alkaline activator**

The compressive strength also decreased as the alkaline activator ratio decreased under the condition of a constant strength index. In the case of B, the decrease in compressive strength was larger when the alkaline activator ratio was less than 15%.

**Strength index**. The relationship between the compressive strength and the strength index of the specimens at the alkaline activator ratio of 15% is shown in **Figure 6**.

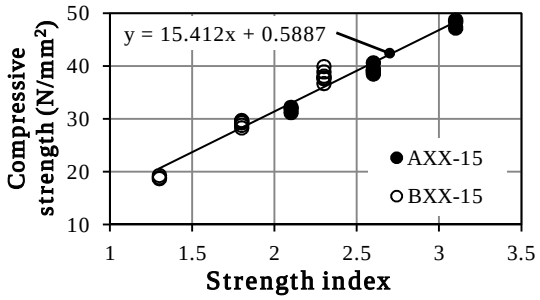


**Figure 6. Relationship between compressive strength and strength index**

The strength index and compressive strength are linearly correlated. The A specimen and B specimen were expressed by the same formula.

**Density**. The density was calculated from the weight and size, which were measured at compressive strength test day 28. The densities of the A specimens and B specimens were approximately 2.4 t/m$^3$ and 2.5 t/m$^3$, respectively. Under the same slump conditions, fine aggregate ratio, and alkaline activator ratio, a higher density is expected because the coarse aggregate content increased and resulted in a low strength index. In this study, the B specimen had a high density of approximately 2.5 t/m$^3$. One reason for this might be that the slag from B had a higher density.

**Shrinkage characteristics**. In case of an alkaline activator ratio of 15%, the test for the change in length was performed based on JIS A 1129 "Methods of test for length change of mortar and concrete." After removal of the form and curing in water for 7 days, the base length is measured. The test results in 20 °C water or in 20 °C air at 60% relative humidity are shown in **Figure 7**.

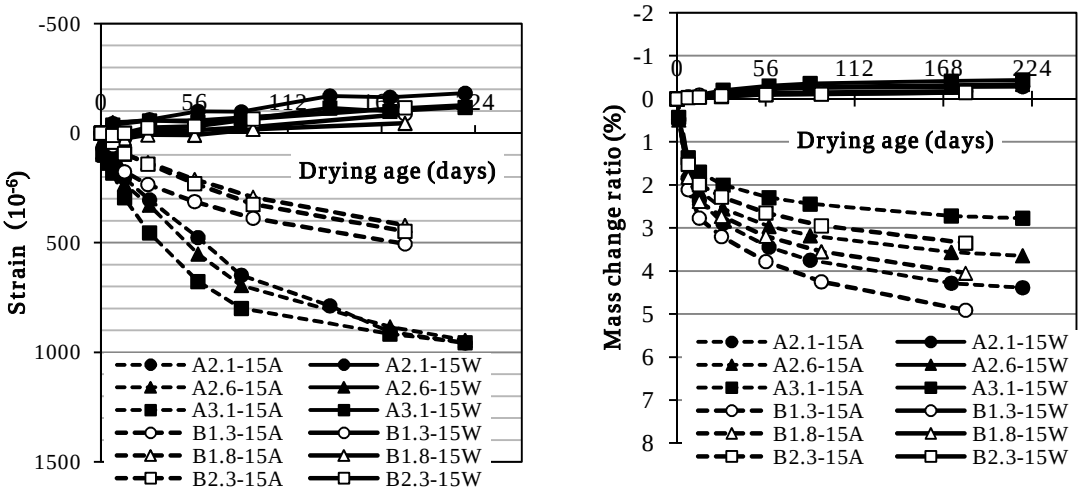


**Figure 7. Result of test of change in length**

In the water case, the progress time was 6 months, and a maximum expansion of approximately 200 μ was observed. In the air case, the A specimen showed about 1,000 μ shrinkage and the B specimen showed about 500 μ shrinkage. Of note is that the shrinkage of the B specimen was not finished at a drying age of 6 months.

**Expansive Soundness**. The expansion soundness test was carried out. As a result, it was found that there were no harmful cracks indicating failure. However, with the A specimens, popout-like surface exfoliation was seen. Moreover, the white sludge was examined around the steel-making slag after exfoliation. Therefore, the included free-CaO or free-MgO in the steel-making slag is considered to be the cause of the exfoliation, which occurred only on the surface. This method entailed curing at 80 °C in water for 10 days. When the temperature is changed to 20 °C, it is supposed that this method corresponds to at least 50 years or more by an engineering manual. Therefore, since the possibility of a harmful crack occurring during the usual in-service period is low, expansion was judged to be sound. It was judged that there was no problem.

**Set characteristics**. Regarding the A specimen cases, the setting time was checked based on JIS A 1147 "Method of test for time of setting of concrete mixtures by penetration resistance." The test results are shown in **Figure 8**. In addition, the initial temperature after mixing was in the range of 17.8–20.5 °C.

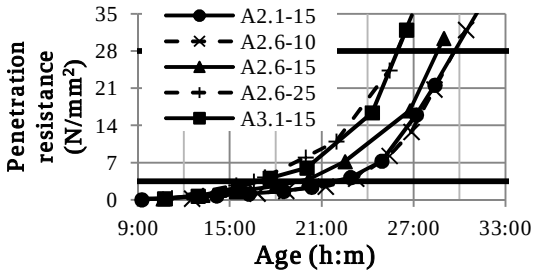


**Figure 8. Results of test for setting time**

In the case of the strength index regularity, the setting time reduced, so the excessive alkaline activator resulted in a high strength index. As compared to ordinary concrete of an ordinary hydrated matrix, the initial setting time increases from 12 h to 18 h. The final setting time becomes about 24 h later. As compared to ordinary anti-washout concrete, the initial setting time increases from 6 h to 12 h. The final setting time becomes about 12 h later.

**Thermal properties**. The test for measuring the adiabatic temperature rise was performed for case A2.6-15. The results of a test for the adiabatic temperature rise and the result from an approximation made using an adiabatic temperature rise characteristic formula by JSCE Guidelines for Concrete and JCI Guidelines for Mass Concrete are shown in **Figure 9** and **Table 4**, respectively. The initial temperature after mixing is 18.0 °C.

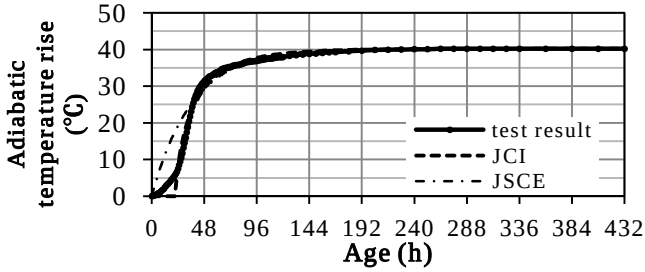


**Figure 9. Results of test for adiabatic temperature rise**

**Table 4. Parameters for adiabatic temperature rise**

| Standard | | JCI | JSCE |
|---|---|---|---|
| Formula of adiabatic temperature rise | | $Q = K[1-\exp\{-\alpha(t-t_0)^{\beta}\}]$ | $T = K\{1-\exp(-\alpha t)\}$ |
| Ultimate adiabatic temperature rise (°C) | K | 40.2 | 40.2 |
| Coefficient for the speed of temperature rise | α | 1.22 | 0.65 |
| Coefficient for the speed of temperature rise | β | 0.73 | - |
| Base of the temperature rise (day) | $t_0$ | 0.9 | - |

The ultimate adiabatic temperature rise of ordinary anti-washout concrete using ordinary Portland cement, a cement content of 400 kg/m$^3$, and W/C = 50% has been reported to be 58.8 °C. It shows that the rise in temperature was reduced by nearly 20 °C. This is one of the key advantages in the case that thermal cracking is considered. Because the setting time is delayed, the initial temperature rise is also delayed. The accuracy possibly improves by using the formula that considers the time delay.

## TRIAL CONSTRUCTION

The steel slag hydrated matrix with anti-washout was applied in a trial construction at a construction site. The slag was used over a total of three days. It was applied as leveling concrete under the culvert box that is installed in the front of the established bulkhead and as back-fill concrete between the established bulkhead and the culvert box after installation. The target slump flow was 550 ± 30 mm, and the target compressive strength was 28 N/mm$^2$ at 28 days. The applied parts and the construction site are shown in **Figure 10**. The mix proportions set up in the trial mixing using a real mixer and agitator truck before construction are shown in **Table 5**.

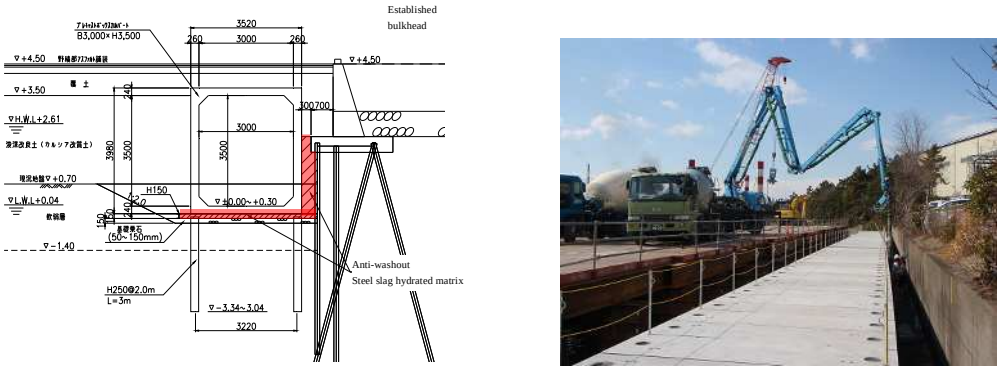


**Figure 10. Applied parts and construction site**

**Table 5. Mix proportions**

| Case | Strength index | Alkaline activator ratio (%) | Unit weight (kg/m$^3$) | | | | | Admixture | |
|---|---|---|---|---|---|---|---|---|---|
| | | | W | BP | OPC | SS | SG | SP(C×%) | Vi(W×%) |
| 1.8-15 | 1.8 | 15 | 245 | 275 | 109 | 812 | 1031 | 2.00 | 1.125 |

During all the days of placing, acceptance inspection revealed that the target slump flow of 550 ± 30 mm was achieved. The compressive strength and expansion soundness of test specimens extracted for the acceptance inspection were also confirmed.

**Flatness and flow inclination**. The flatness without vibrations and flow inclination were measured while placing the steel slag hydrated matrix with anti-washout by using a concrete pump. Here, the flatness was defined as crown flatness after placing only the moving flexible hose of the concrete pump without vibrations. The flow inclination was defined as the inclination measured in the range that flowed from the tip of the flexible hose after placing

without moving the flexible hose of the concrete pump or without vibrations. The results of the measurement are shown in **Figure 11**

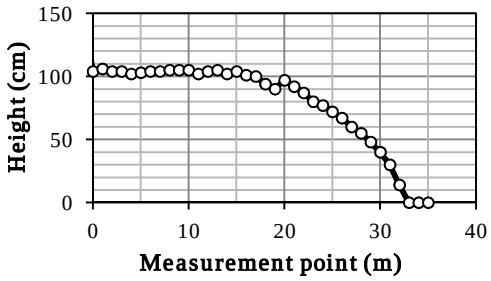


**Figure 11. Flatness and flow inclination**

The flatness was calculated from the results of the measurement points at 0–10 m. The maximum vertical interval was 40 mm. The flow inclination of the measurement points at 20–35 m was 12%.

## CARBON-DIOXIDE EMISSIONS

The carbon-dioxide emissions of ordinary anti-washout concrete and anti-washout steel slag hydrated matrix were determined. In the mix proportions, the water content and slump flow were 230 kg/m$^3$ and 550 ± 30 mm, respectively. In addition, the compressive strength at 28 days was almost the same. The mix proportions and estimated results are listed in **Table 6**.

**Table 6. Estimated results of carbon-dioxide emissions**

| Item | Generating unit (g-$CO_2$/kg) | Anti-washout concrete | | Anti-washout steel slag hydrated matrix | |
|---|---|---|---|---|---|
| | | Unit weight (kg/m$^3$) | Generating quantity (kg-$CO_2$) | Unit weight (kg/m$^3$) | Generating quantity (kg-$CO_2$) |
| W | 0 | 230 | 0 | 230 | 0 |
| OPC | 757.9 | 383 | 290275.7 | 0 | 0 |
| Sand | 3.5 | 640 | 2240 | 0 | 0 |
| Gravel | 2.8 | 1010 | 2828 | 0 | 0 |
| BB | 460 | 0 | 0 | 119 | 54740 |
| $BP_B$ | 24.1 | 0 | 0 | 301 | 7254.1 |
| $SS_B$ | 2.6 | 0 | 0 | 910 | 2366 |
| $SG_B$ | 2.6 | 0 | 0 | 947 | 2462.2 |
| SP | 150 | 4.125 | 618.8 | 10.50 | 1575 |
| Vi | - | 2.53 | - | 2.53 | - |
| total | - | - | 295962 | - | 68397 |

The carbon-dioxide emissions of the anti-washout steel slag hydrated matrix were 25% of those of the anti-washout concrete. This is largely attributed to the reduced cement content in the former.

## CONCLUSIONS

In the development of steel slag hydrated matrix with anti-washout performance, the results of the laboratory test, trial construction, and estimation of the carbon-dioxide emissions are as follows.

- In this test range and construction range, the problem of anti-washout steel slag hydrated matrix was not checked.
- The Young's modulus of the developed matrix is approximately 75% that of ordinary concrete.
- With the alkaline activator ratio in the 0–25% range, there is a tendency for compressive strength to also be high. The decrease in compressive strength may be large when this ratio is less than 15%.
- The strength index and compressive strength are linearly correlated.
- The density of the matrix is larger than that of ordinary concrete and is expected to be 2.4–2.5 $t/m^3$.
- The shrinkage characteristics may change drastically with the materials used. When it is underwater, some expansion behavior is observed.
- In the expansion soundness test, depending on the material to be used, popout-like exfoliation considered to be satisfactory on the usual conditions may occur only on the surface.
- Setting is delayed. In this case, the initial setting time was more than 15 h, and the final setting time was more than 24 h.
- In case A2.6-15, the ultimate adiabatic temperature rise was lower than that of ordinary anti-washout concrete by approximately 20 °C.
- During construction by concrete pump, in the case of a slump flow of 550 mm, the flatness was 40 mm in the maximum vertical interval. Flow inclination was approximately 12%.
- Carbon-dioxide emission is approximately 25% that of ordinary anti-washout concrete.

Anti-washout steel slag hydrated matrix has advantages, such as high density or smaller temperature rise. If these points are taken into consideration, the anti-washout steel slag hydrated matrix can be used as an alternate to anti-washout concrete. Owing to the advantages of effective use of resources and reducing carbon-dioxide emissions, this material is expected to have wide applicability.

## REFERENCES

Coastal Development Institute of Technology (CDIT). (2008). "Technical Manual for Steel Slag Hydrated Matrix." Library of Coastal Technology, No.28 (in Japanese).

Matsunaga, H. et al. (2003). "Basic Characteristics and Organism Adhesion in the Marine Environment of Steel Slag Hydrated Matrix." Iron and Steel, Vol.89, No.4, 454-460 (in Japanese).

Takahashi, R. and Hamada, H. (2006). "Mechanical Properties of Steel Slag Hydrated Matrix with Flexural Strength $5N/mm^2$ Level." Proceedings of Annual Convention of the Japan Concrete Institute, Vol.28, No.1, 1613-1618 (in Japanese).